Paper 41

Alturas: A Unique Discovery Within a Mature District Through Integrating Sound Geological Practices, Multidisciplinary Expertise and Leading Technology

Astorga, D. [1], Griffiths, S. [2], Crosato, S. [2], Jorquera, C. [2], Plasencia, C. [3]

1. Compania Minera Salitrales Ltda., Chile
2. Inversiones Barrick Conosur Ltda., Chile
3. Minera Barrick Misquichilca, S.A., Peru

ABSTRACT

Discovery of a high-sulfidation epithermal system at Alturas represents the culmination of over 30 years of geological understanding combined with the application and integration of multi-disciplinary geoscientific techniques at all exploration stages and scales.

The Alturas deposit is located in the gold-rich El Indio belt of central-northern Chile. The belt is defined by the overlap of two prolific magmatic belts; the Eocene-Oligocene in the north and the Miocene in the south, both of which host multiple world class (porphyry copper) deposits. El Indio belt has been the focus of over 30 years of exploration by many experienced explorers, resulting in a series of world class gold discoveries. These discoveries have evolved from outcropping high sulfidation veins (El Indio-Tambo, 1976 discovery), to basement granite hosted deposits (Pascua Lama, 1995 discovery), to felsic volcanic hosted disseminated deposits (Veladero, 1998 discovery) and most recently the semi-concealed Alturas deposit, announced in 2015, reflecting the global trend towards concealed discoveries. Over the exploration history, the knowledge of the belt and the deposit types has evolved and the lessons learned reapplied, which culminated in the Alturas discovery.

A dedicated, methodical, multi-year exploration campaign commenced in 2010 to re-evaluate the economic potential of this prospective, yet perceived mature, 150 km long belt. This commenced with a belt wide 1:25,000 geological mapping campaign and the generation of 42 systematic (2 km spaced) transects. Combined with remote sensing (multi- and hyper-spectral), regional magnetic surveys and targeted geochronology, a three-dimensional compilation generated 19 geologically-defined targets, with Alturas being the top ranking of the high sulfidation targets. Following this regional campaign, a targeted program of geological mapping over 10 square kilometers, supported by spectral, geochemical and geophysical data acquisition, defined individually subtle anomalies which, when integrated into a conceptual geological model, collectively provided a compelling case for a concealed target. From the onset of drilling, innovative technology was incorporated, including digital collection of geological data (surface and drill core), core scanning (high resolution photography, hyperspectral imagery and geotechnical data), portable x-ray fluorescence (pXRF) analyzers and optical high resolution imagery of drill hole walls. These data sets were integrated to generate a robust three-dimensional geological model which to date has supported the delineation of a 6.8 Moz inferred gold resource (Barrick, 2017).

INTRODUCTION

Alturas is a high sulfidation (Hedenquist, 1987) epithermal Au deposit located approximately 220 km east of the coastal city of La Serena (Figure 1). Discovery of strong and continuous oxidized gold and silver mineralization at the project, currently subject of a scoping study, was announced in April 2015. In the five years preceding this announcement, Alturas project progressed through target delineation, drill testing and advanced exploration stages after being highlighted as a top-ranked opportunity during grassroots activities which were initiated in 2010.

Alturas is located in El Indio Belt (EIB), an approximately 150 x 20 km, north-south trending zone in the high Andes. The EIB represents one of the most fertile and well mineralized districts in the world, evidenced by Alturas (6.8 Moz Au; Barrick, 2017) and other deposits such as Pascua-Lama, Veladero and El Indio-Tambo (see Table 1). Currently known gold mineralization is distributed over multiple mineralizing events (Bissig et al, 2015), mainly in high-sulfidation deposits.

Geochronological data show that the extensions of major porphyry Cu belts of Chile (Eocene – Oligocene and Upper Miocene in age) overlap in EIB. Here, mineralization is related to compressional tectonics, uplift and crustal thickening over an area of flat subduction (Ramos and Folguera, 2009). High sulfidation systems of the Andes are located in these zones and distributed in clusters within longitudinally restricted segments from their host arcs, associated with low volume volcanism confined to isolated eruptive centers (Jannas et al., 1999; Bissig, 2015). These deposits form at depths of less than 1 km and mineralizing processes are influenced by relatively near surface physio-chemical conditions (Sillitoe, 1999; Sillitoe and Hedenquist, 2003' Heinrich, 2007).

El Indio Belt has been a focus of exploration for over 30 years by companies such as Saint Joe, Bond Gold, Lac Minerals, Homestake and Barrick (Jannas et al., 1999), resulting in a series of significant gold discoveries. These discoveries have evolved

In "Proceedings of Exploration 17: Sixth Decennial International Conference on Mineral Exploration" edited by V. Tschirhart and M.D. Thomas, 2017, p. 587–600

from outcropping high sulfidation veins (El Indio, 1976 discovery) to hydrothermal injection breccias (Tambo, 1982 discovery) to basement granite hosted deposits (Pascua Lama, 1995 discovery) to felsic volcanic hosted disseminated deposits (Veladero, 1998 discovery) and most recently the semi-concealed Alturas deposit, announced in 2015 (Figure 2). This reflects the global trend towards concealed discoveries. Over the years, geological knowledge of the belt and the contained deposit types has evolved and lessons learned from early discoveries re-applied, which has culminated in the Alturas discovery. In short, this greenfields discovery resulted from a methodical and focused multi-disciplinary exploration effort, in what would have previously been described as mature exploration ground.

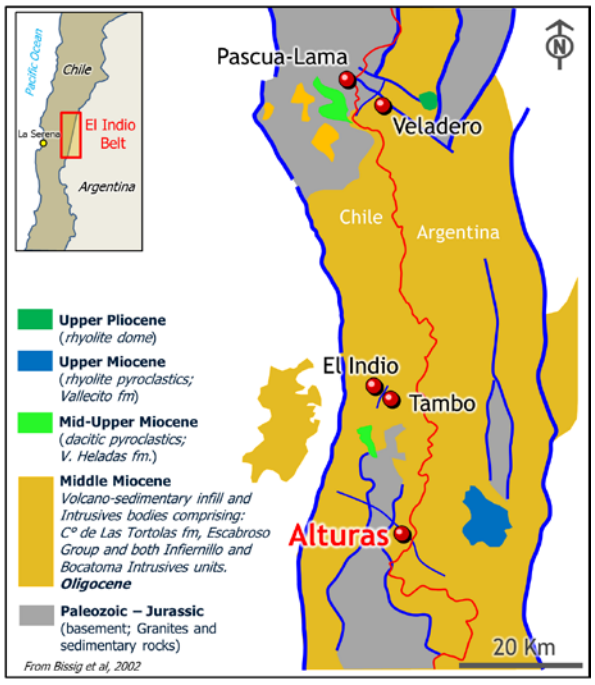

Figure 1: Alturas location map and simplified geology of EIB with location of other high sulphidation deposits (red dots). Major faults marked by blue lines, international border as red line; inset shows location in Chile. Modified from Bissig et al. 2014.

Commencing 2010, a multi-disciplinary exploration program sought to re-evaluate the economic potential of EIB. The 'maturity clock' was re-set by considering new potential host rocks and mineralization ages to build a robust pipeline of targets warranting drill testing. Firstly, a belt wide 1:25,000 grassroots geological mapping campaign, comprising 42 systematic (2 km spaced) transects, focused on defining the

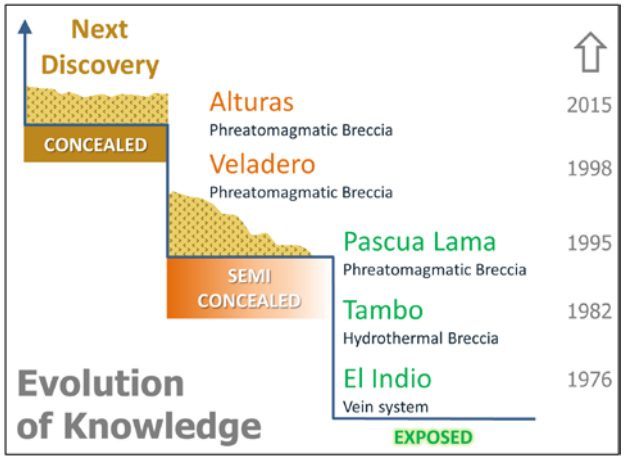

Figure 2: Greenfields discoveries in EIB over time, illustrating evolution of geological knowledge (different settings) and decreasing level of exposure from right to left from outcropping to concealed deposits.

	El Indio	Tambo	Pascua Lama	Veladero	Alturas
					
Discovery	1976	1982	1995	1998	2015
					
Type	High sulphidation (sulphide ore). Multi-Vein deposit with high-grade gold (DSO) and Cu-Au veins	High sulphidation oxide deposit related with hydrothermal injection breccia and quartz+barite veins	High sulphidation oxide/sulfide deposit	High sulphidation oxide deposit	High sulphidation oxide deposit
Prod. Statistics	**4.5 Moz Au**, 24 Moz Ag & 472K tons Cu (over 23 years)	**1.5 Moz Au** (over 17 years)	–	2016 Production **544 Koz Au**	–
2016 Reserves/ Resources			Total Reserves **14.05 Moz[1] Au** (1.57g/t, 278M tonnes) Proven Reserves: 1.8 Moz[1] Au (1.94g/t, 29M tonnes) Probable Reserves: 12.2 Moz[1] Au (1.53g/t, 249M tonnes)	Total Reserves **6.7 Moz[1] Au** (0.83g/t, 252M tonnes) Proven Reserves: 602 Koz[1] Au (0.78g/t, 24M tonnes) Probable Reserves: 6.1 Moz[1] Au (0.84g/t, 228M tonnes)	Inferred Resource: **6.8 Moz[1] Au** (1.0 g/t, 211M tonnes)
Current Status	Closed (since 2002)	Closed (since 1999)	Pre-Feasibility (Lama)	Producing (since 2005)	Scoping Study

Table 1: Au deposits of EIB with production and reserve/resource statistics.
[1] – as reported in Barrick, 2017.

structural architecture and tectonic evolution of the area (Figure 3). This geological framework was combined with reprocessed remote sensing (multi- and hyper-spectral), regional aeromagnetic surveys and strategic geochronology samples, resulting in the emergence of 19 target areas, with Alturas being the top-ranked high sulfidation target.

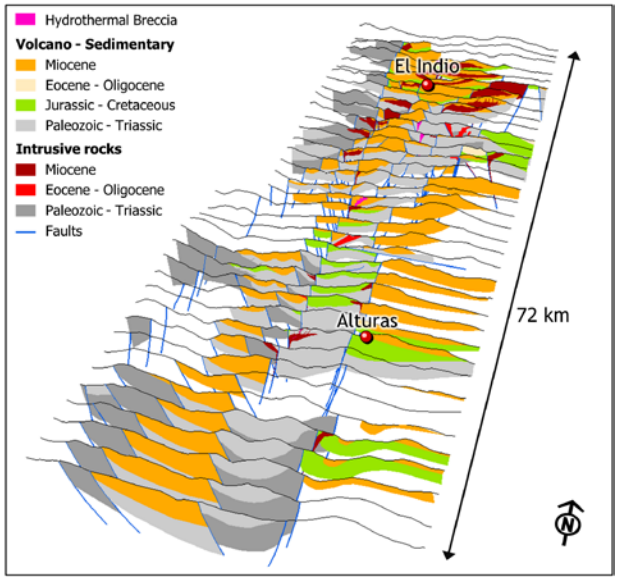

Figure 3: Grassroots stage (1:25,000 scale) structural geology sections at 2 km spacing which were used to interpret the structural architecture of the EIB.

Following this regional campaign, a target delineation program comprising geological mapping over 10 square kilometers was supported by geochemical, geophysical and spectral data acquisition. Individual subtle anomalies were defined which, when integrated into a conceptual geological model, collectively provided a compelling case for a concealed drill target. In order to further understand the geology, successfully target and ultimately discover the Alturas deposit, exploration activities resulting in a systematic reduction in scales from grassroots to advanced exploration drilling have incorporated several technologies focused on solving specific technical challenges. For example, high-resolution hyperspectral core scanning aided in interpretation of deposit paragenesis and in-situ down hole imaging systems provided insight into the detailed structure.

ALTURAS GEOLOGY

Alturas is an oxidized high sulfidation epithermal system hosted in a mid- to upper-Miocene volcanic and volcanoclastic sequence of dacitic composition. The deposit is spatially associated with multiple, coalescing phreatomagmatic breccia centers which form a diatreme complex 500 x 500 x 300 m in size (Figure 4). The hydrothermal alteration zone is 3 x 3 km in extent and characterized by advanced argillic alteration, typical of high-sulfidation Au deposits (Sillitoe and Hedenquist, 2003). At Alturas alteration is zoned from vuggy silica (residual silica) in the center of a quartz-alunite envelope, overprinted by several subsequent silicification events. In lateral and higher parts of the system alteration is characterized by a kaolinite–dickite–alunite-

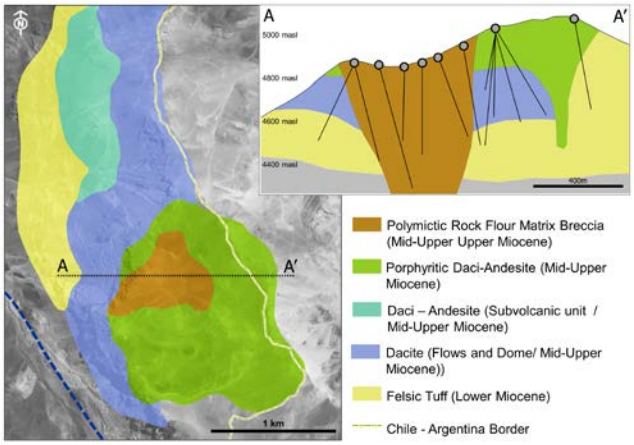

Figure 4: Lithological map and conceptual section showing spatial relationships between main Alturas host (dacitic tuffs of lower Miocene Tilito Fm.), dacite flows and domes (middle to upper Miocene), and phreatomagmatic breccia. Location of cross-section shown as broken line A-A'.

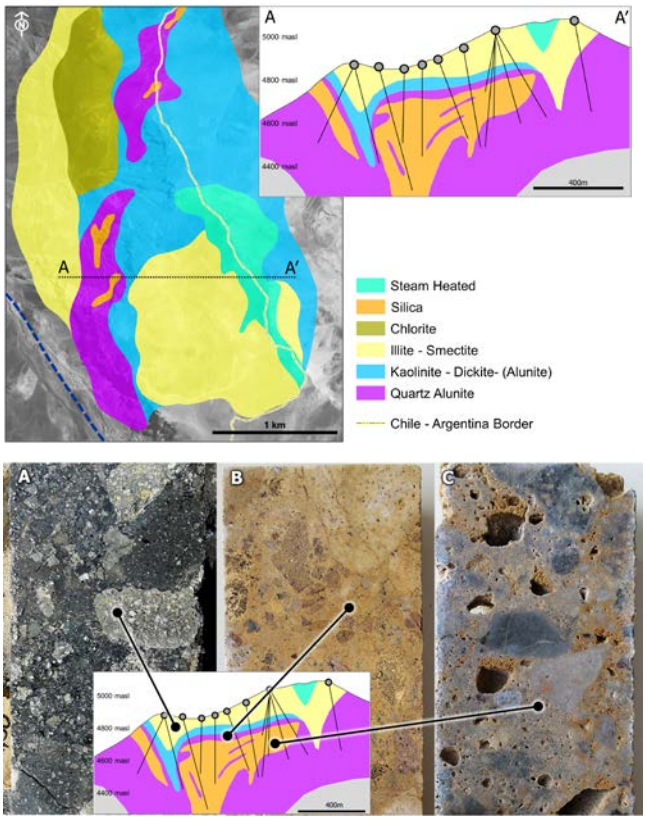

Figure 5: Alteration map and conceptual section showing spatial relationships between main Alturas alteration assemblages. Mineralization occurs with silicification events. Location of cross-section shown as broken line A-A'. Photographs illustrate key alteration in breccias – a) illite-smectite-pyrite; b) quartz-alunite; c) silicification occurring as 'silice parda.

illite/smectite assemblage. The shallowest part of the system exhibits 'steam heated' alteration which is powdery in nature and composed of micro-crystalline quartz, alunite and kaolinite (Figure 5).

Gold-silver mineralization is associated with distinct silicification events which overprint phreatomagmatic breccias and their contacts and host rocks at depths of 100 – 200 m below surface. Evidence of mineralization on the surface is scarce due to a high degree of preservation of the hydrothermal system. Upper parts of the system are dominated by kaolinite–dickite–alunite-illite/smectite, without anomalous values of Au-Ag. The only exception to this is a silicified cliff which is exposed at the same elevation as Au mineralization in the deposit (Figure 5). Mineralization and silicification show a very good correlation to resistivity highs, as measured by electrical geophysics (discussed later in this paper).

GEOLOGICAL MAPPING AND LOGGING

Geoscientific data collection at distinct scales resulted from progressing through a disciplined, phased exploration program from grassroots to advanced exploration. Each stage focused on evaluation of potential for the presence of key indicators of a mineral system. At the grassroots stage emphasis was given to defining regional stratigraphy through recognition of intrusive, volcanic and sedimentary units, their contact relationships and absolute ages. A regional structural framework was also generated with 1:25,000 scale geological mapping and systematic cross-sections spaced 2 km apart.

Target delineation work resulted in a 1:2,500 scale geological map of the project area with a focus on identifying evidence for high sulfidation mineralization such as magmatic and phreatomagmatic centers, typical sulfide and alteration mineral assemblages, erosional level and a more detailed structural understanding of the system. Drill testing and advanced exploration were supported by continued surface geological mapping and sampling at 1:1,000 and 1:500 scales and core logging. Characterization of project specific lithological variations allowed recognition that discrete volcanic and volcano-sedimentary facies define a diatreme breccia complex that was subjected to several phases of hydrothermal alteration. These criteria were documented to ensure standardized data capture and a robust geological interpretation.

Surface and drill hole geoscientific data were interpreted to generate a series of surface and sub-surface plans and cross-sections illustrating lithology, alteration and mineralization at 200 m and 100 m intervals at drill testing and advanced exploration stages, respectively. Integration of these 3D interpretations contributed to generating a geological model focused on identifying controls on, and continuity of, Au mineralization.

Key geological data and supporting technical information was digitally captured during all scales of exploration, from grassroots to target delineation, to drill testing and advanced exploration. Rugged portable computers and tablets were used for field data capture, with data regularly backed up on office-based servers. Also, the use of software applications facilitated generating 2D and 3D geological maps and models (Figure 6), which are fundamental tools for data visualization.

Geochronology, for example U-Pb of zircon for dating lithology and Ar-Ar and K-Ar methods in alunite to date alteration, was also applied at different stages of the program. During grassroots exploration these techniques provided information which assisted in the compilation of an accurate stratigraphic column of EIB. At target delineation and drill testing stages geochronology permitted characterization of the evolution of distinct deposition events in volcanic sequences, dome complexes, pyroclastic rocks and phreatomagmatism (Figure 7). Multiple advanced argillic alteration and silification events associated with mineralization were also distinguished with geochronological support.

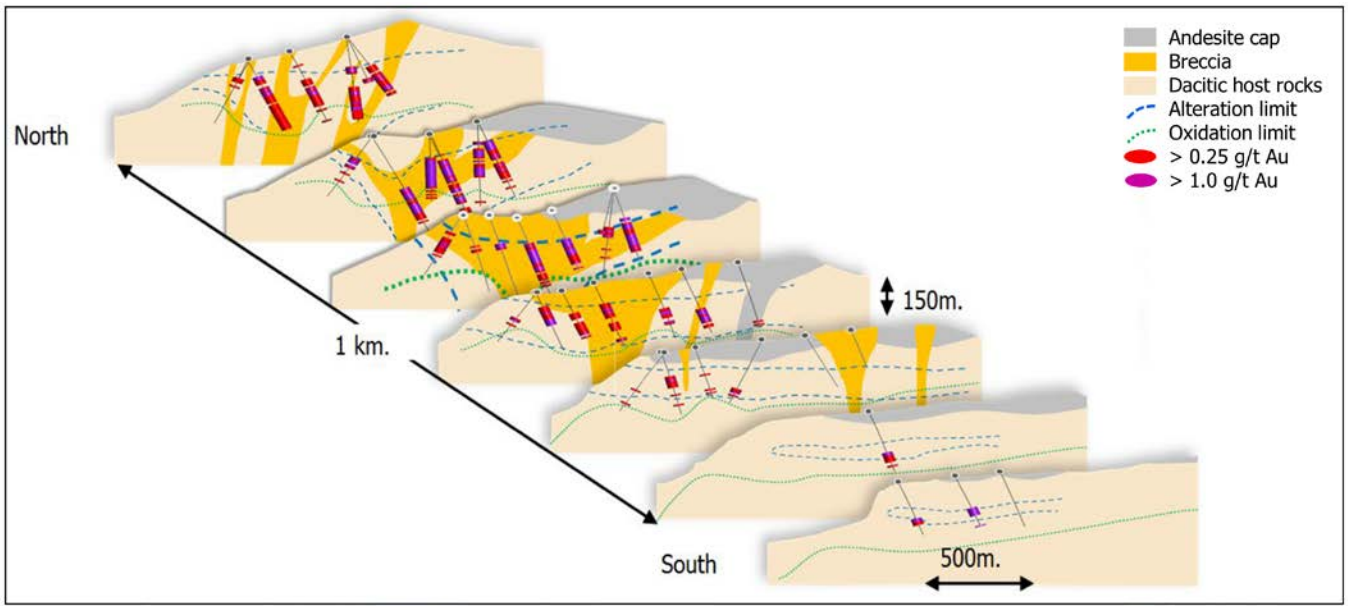

Figure 6: Simplified stacked geological cross-sections showing main lithological units and continuity of oxidized Au mineralization. A phreatomagmatic breccia body and its margins represent an important control on mineralization.

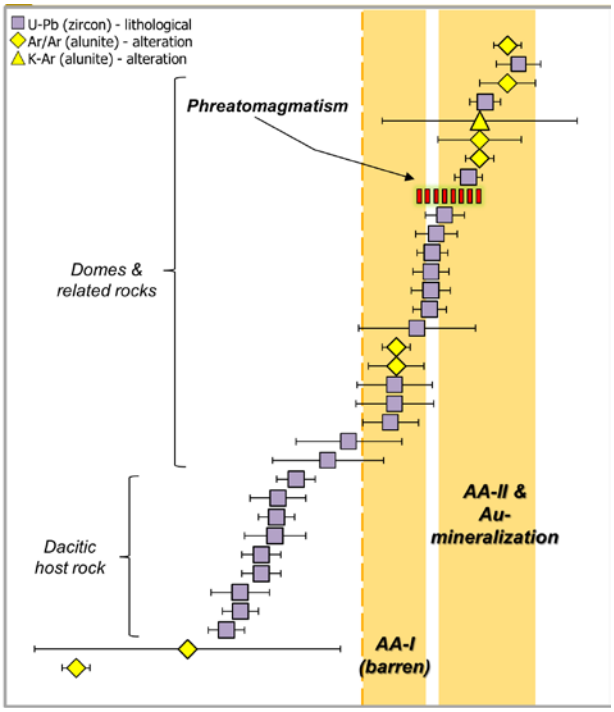

Figure 7: Graphic illustration of extensive geochronological data from lithologies and alteration which define evolution of the Alturas magmatic-hydrothermal system. AAI – Advanced Argillic phase I, AAII - Advanced Argillic phase II.

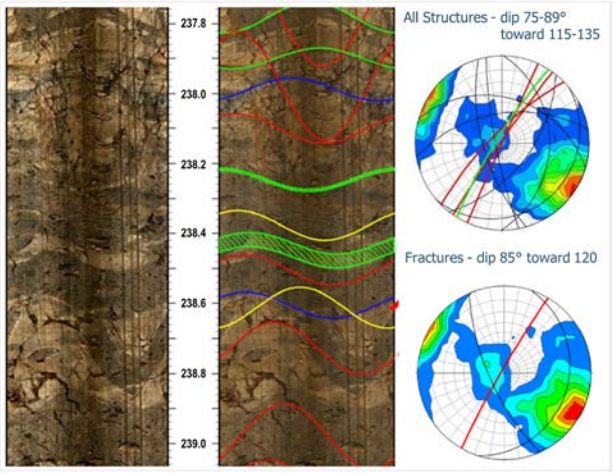

Figure 8: Televiewer images (left and center) and stereonets (right) showing main structural orientations. Red lines on center image correspond to fractures on stereonets. Green, yellow and blue lines highlight other planes identified in the interpretation of the televiewer data.

At the drill testing and advanced exploration stages, use of an optical televiewer instrument enabled logging of oriented structural observations. The optical televiewer captures high-resolution down-hole images using a system of rotating conical mirrors; data are captured in the form of real color digital images (Figure 8). Analysis and interpretation of orientated structural data, combined with surface mapping, resulted in validation of the structural model, orientation of controls on mineralization and optimization of the ongoing exploration program (Figure 8).

A high spatial resolution (0.05 mm / 50 µm) hyper-spectral core scanning instrument (Corescan) was installed on-site in the core yard. Corescan generates digital mineral and mineral assemblage maps and provides geotechnical information (e.g. Rock Quality Data, RQD). This technology was implemented throughout the drill testing and advanced exploration stages. Analysis and interpretation of resulting data has been fundamental in understanding geological relationships and generating a 3D geological model of the deposit. This model includes spatial distribution of various alteration assemblages, which where certain overprinting relationships are interpreted, assist in understanding of the timing of these events (see following section for more detail).

SPECTRAL GEOLOGY & REMOTE SENSING

At the grassroots stage, alteration maps were generated from a Probe 1 airborne hyperspectral survey (126 band sensor covering VNIR and SWIR, 8 x 8 m pixels) conducted over EIB in the 1999-2000 field season. Reprocessing of this survey was calibrated using outcrops with known (mapped) alteration as 'training points.' High spatial and spectral resolution allowed the mapping and differentiation of K-alunite and Na-alunite. Kaolinite, illite, dickite and pyrophyllite were also discerned, although the instrument did not map silica as the thermal range is outside the bandwidth of Probe 1. This tool was very useful for identifying areas of advanced argillic alteration for follow-up which were associated with subtle regional stream sediment geochemical anomalies (see following section for more detail), one of which was present at Alturas.

Satellite mounted multispectral technology such as ASTER (Advanced Spaceborne Thermal Emission and Reflection Radiometer) with 14 bands (3 VNIR, 6 SWIR and 5 TIR) aided in rapidly prioritizing exploration work during the grassroots stage. Spectral mapping of advanced argillic alteration associated with silicification (e.g. aforementioned silica cliff) identified areas of interest within EIB. Again, one of these areas of interest was near Alturas which ranked it highly for follow-up exploration.

At the target delineation stage of exploration, the Crosstalk correction (ERSDAC, 2003) and an atmospheric calibration (ACORN 7a) were applied to Level 1B ASTER images in order to generate a more robust alteration map. This identified a central area with silica, surrounded by advanced argillic alteration with prominent alunite, bordered by an argillic alteration zone composed of high-Al illite (Figure 9). This zonation was field-validated resulting in an almost 100% verification of the ASTER interpretation.

Portable hyperspectral instruments such as ASD FieldSpec and ASD TerraSpec were also employed during the various exploration stages. This technology was used to assist in validation of ASTER anomalies and to generate field based alteration maps. A series of protocols were developed for sample

collection whereby a corresponding spectral sample was obtained at every geochemical sample site. These samples were systematically analysed using an ASD unit by company personnel, data being captured and stored using digital platforms. Additional to capturing individual spectra, metadata were recorded regarding mode of mineral occurrence, which was used to interpret paragenesis of individual alteration events (Figure 10). We consider this an example of 'Best Practice' in the application of spectral data to mineral exploration.

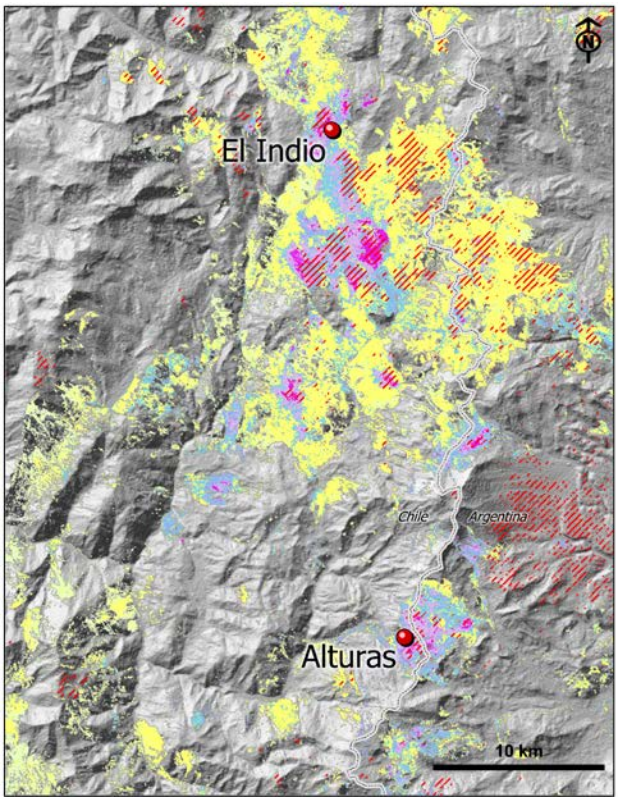

Figure 9: ASTER interpreted alteration map of EIB. Intense alunite at the core of Alturas and El Indio appears magenta; alunite-kaolinite pink; kaolinite-weak alunite light blue; and high-Al illite yellow. Strong silicification is shown as red hachured.

Software such as ENVI, SpecMin, ViewSpecPro and The Spectral Geologist (TSG) and guides such as GMEX (AusSpec, 2012) were used to interpret spectral data. Interpretations resulted in identification of mineral composition vectors in alunite and illite, indicating proximity to geochemical anomalies and other spatial relationships with subtle Au anomalism on surface. During drill testing it was found that the nature of these spectral parameters in semi-covered areas, identified during target delineation, were repeated at depth. This analysis and interpretation of surface and down-hole spectral data resulted in the identification of several important deposit characteristics, such as:

- K-alunite is a good indicator of proximity to Au anomalies, either on the surface or below (Figure 10). This is similar to alunite found at Pascua-Lama and Veladero. Alunite which is very high in K was identified close to high grade Au mineralization.
- Low crystallinity, high Al-illite is found in areas of geochemically anomalous Al and is thought to be indicative of highly acidic conditions present during an early argillic alteration event (Figure 10).

As previously mentioned, Corescan was applied to drill core during the drill testing and advanced exploration stages. This hyperspectral scanner generates images of high spatial and spectral resolution, e.g. photographic core images at 50 µm, hyperspectral images at 500 µm with a spectral range of 450 nm to 2,500 nm at 4 nm resolution. Images resulting from scanning the core provided high-impact, real-time assistance in geological logging through improved consistency in alteration mineral and mineral assemblage identification. Combining clay mineralogy with texture and mode of occurrence assisted in the interpretation of mineral paragenesis (Figure 11) and hence the generation of a robust 3D alteration model. Corescan also output a semi-quantitative estimation of RQD (automated geotechnical logging).

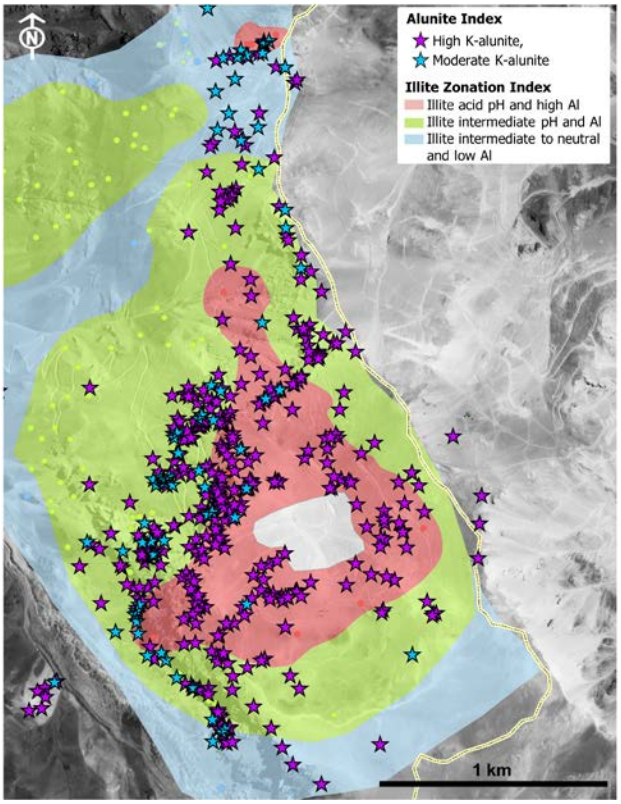

Figure 10: Image showing Alturas project-scale alunite distribution (colored stars) relative to illite zonation (colored areas). K-alunite (blue stars) is peripheral to very high K-alunite (purple stars). Here, this distribution coincides with a zonation from neutral pH, low Al-illite to progressively more acidic, higher Al-illite.

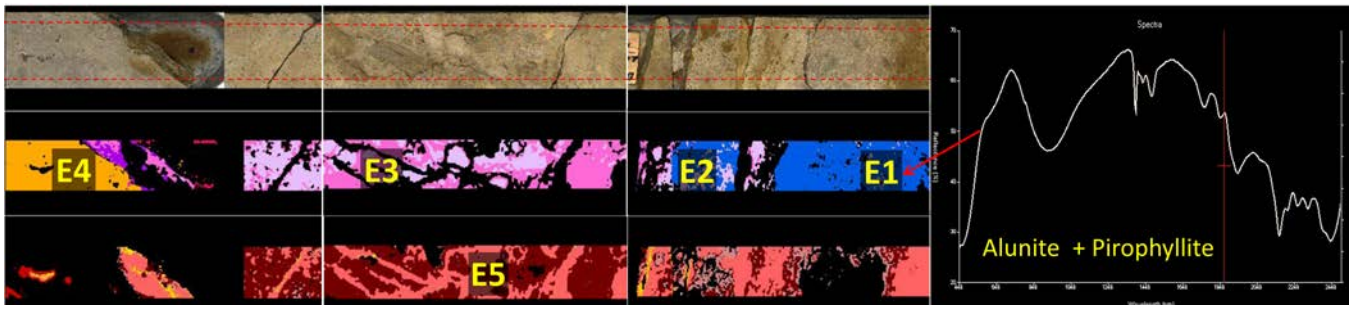

Figure 11: CoreScan output with interpreted alteration paragenesis. E1: pyrophillite + Na-alunite in breccia matrix, clasts and cavity-filling. E2: pyrophillite + dickite + K-alunite. E3: K-alunite + silica in breccia matrix and clasts. E4: silica in breccia matrix (mineralized event). E5: jarosite in cavities and fracture-filling. Spectra curve shown to right.

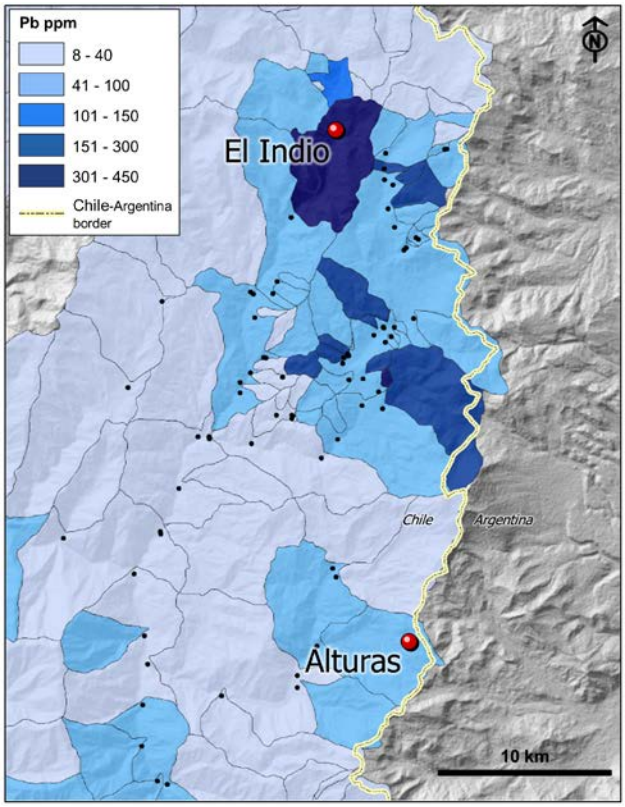

Figure 12: Distribution of Pb in EIB stream sediment sample basins. Sample locations are indicated by black dots. Subtle concentrations of Pb occur in Alturas drainage basins, as compared to those near El Indio.

An important part of the process of applying Corescan technology was working in partnership between Barrick and Corescan technical specialists and project geologists. Firstly, a set of protocols for systematic data capture was documented. Then a series of additional data fields were established in order to capture deposit-specific spectral parameters, such as alunite and illite composition indices at certain wavelengths and reflectance (spectra depth) of jarosite. These features add to the understanding of different alteration events at Alturas. Similarly, as part of a process of continual improvement, alteration assemblage "class maps" (Corbett and Leach, 1998; Camuti, 2008) were implemented.

Based on project needs, Corescan provided several data visualization platforms such as Coreshed (via web), Product Viewer (tablet compatible), acQuire NEO and CoreViewer (Figure 11). Linked to the main project acQuire database, acQuire NEO allowed visualization of integrated geology, alteration and geochemical data. The CoreViewer platform enabled Barrick technical specialists to review spectral data quality control remotely.

Another deliverable from Corescan was a numerical log containing mineral abundances and compositional and crystallinity indices, among other parameters. These data were then exported for integration with geology and geochemistry and used in modeling software such as Leapfrog and Target (Arc/GIS) to support interpretation of cross-sections, level plans and 3D deposit models. As such, ongoing development in the understanding of distinct alteration and mineralization events led to further characterization of fertile levels in the mineral system and spectral and geochemical vectors to ore.

GEOCHEMISTRY

Appropriate geochemical strategies and techniques were applied at the various stages of the project pipeline, resulting in a series of sampling programs from grassroots (regional) to target delineation (local) scales. A grassroots stream sediment survey was conducted with a sampling density of 1 sample per 20 km^2 (Figure 12). The survey was designed according to topography and the mineralization type sought, which at the time of sample collection (1999) was epithermal and porphyry style. At each sample site two samples were sieved to <2 mm, one to analyze the <106 µm fraction for Au by fire assay with AAS finish and multi-element determination by four acid/aqua-regia digestions with ICP-MS finish. The second sample from each site was analysed for Au by BLEG. The approximately 400 samples from this survey (and all subsequent samples taken from the project) were analysed at internationally certified laboratories complying with ISO standards. These historical stream sediment data were re-interpreted considering other criteria such as structural domains, alteration ages, host rocks and alteration type for ranking and definition of prospective areas in 2010. Although Au results were not conclusive, other elements such as Pb indicated some mineral potential in the prospective blocks.

Multi-element anomalies in structural blocks with potential to preserve epithermal deposits were followed-up as part of target

delineation work (at camp scale) with both systematic and "character" rock chip sampling in 2011. In Alturas camp, sampling was carried out on a 100 x 100 m north-west oriented grid and reconnaissance rock chip samples were collected by geologists during 1:2,500 and 1:1,000 scale geological mapping. Samples were analysed for Au by fire assay in (50 g aliquot) with AAS finish and multi-element determination by four acid digestion and ICP-MS. Volatile elements (As, Sb, Se, Te and Tl) were determined by aqua-regia digestion and ICP-MS finish, and Hg by cold vapor with AAS finish.

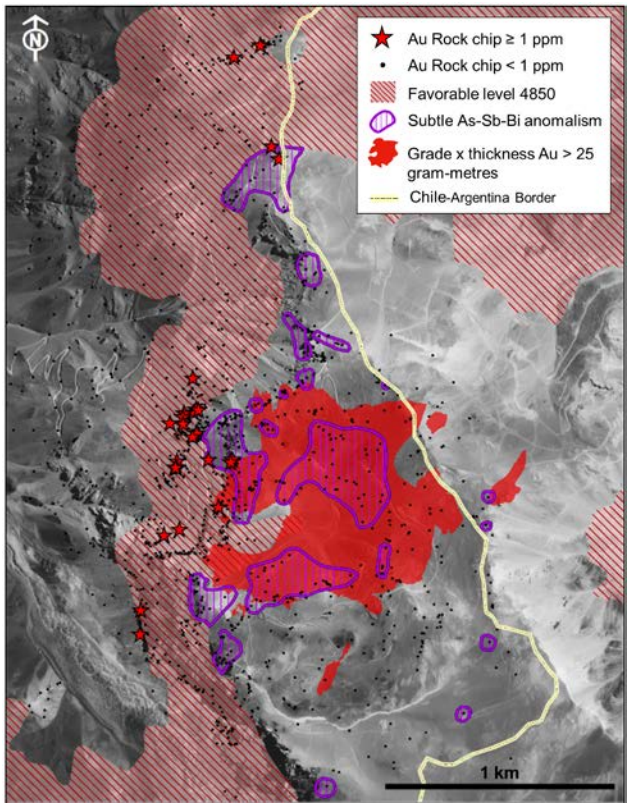

Figure 13: Alturas project-scale distribution of ≥1 ppm Au (red stars) which highlights an outcropping favourable horizon for mineralization at the western silicified cliff. Grade-thickness >25 gram-meters from drilling is shown in the red shaded area. Subtle volatile element anomalies in rock chips are outlined by purple hachured areas.

Rock chip data were critical for identifying a favorable horizon for mineralization (defined by values >0.1 ppm Au) which highlighted a Au-bearing outcrop in the west (aforementioned silicified cliff), containing several samples reporting >1 ppm Au (Figure 13). However, concentrations of Au and pathfinder elements (As, Sb, Hg, Bi) were very low where the deposit is covered. A study of surface geochemistry at another Barrick high sulfidation system (Veladero) was carried out and compared to rock chip data from Alturas which resulted in recognition of very similar ranges of volatile elements. Subtle concentrations of Au in the order of tens of ppb and volatiles such as As, Sb and Bi were recognized in alunite bearing tuff. This was interpreted as a manifestation of potentially blind mineralization, which was borne out by subsequent drill testing (Figure 14).

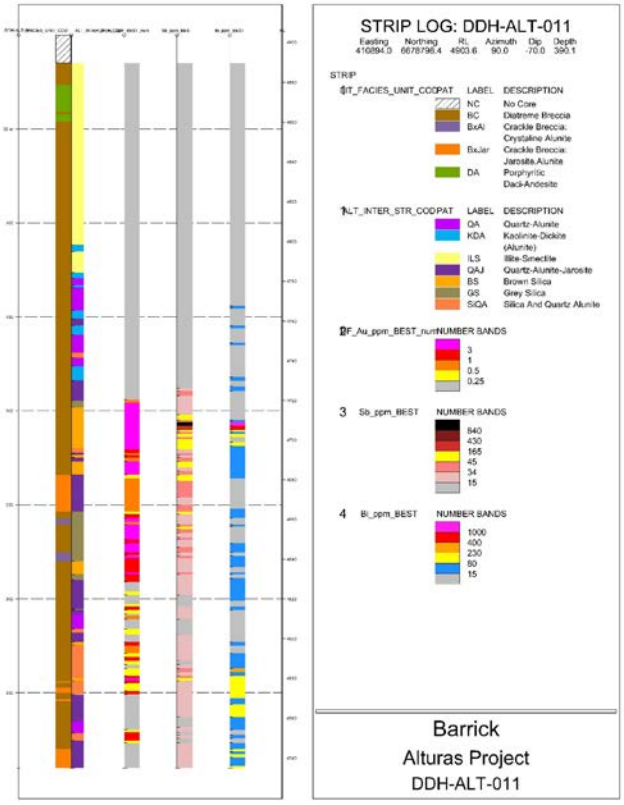

Figure 14: Striplog illustrating lithological influence on alteration (a) and related Au mineralization (b). Note association between Au mineralization, occurrence of silica and Sb and Bi anomalism.

Drill testing of the most favorable anomalies commenced early 2012. HQ diameter (63 mm) core samples averaged 3-4 kg and were analysed by the same methods as rock chips. Initial drill results returned some samples >1 g/t Au, similar to the abovementioned Au-bearing silicified cliff. This was interpreted as being related to silicification at a favorable horizon in a phreatomagmatic breccia. Consequently, a barren cover of approximately 100-150 m was recognized over the center of the mineralized zone, thus reinforcing the concept of a largely concealed target. These results, along with layers of information derived from other disciplines, helped target further drilling during advanced exploration.

Drill hole sampling procedures rapidly developed into a systematic approach and were documented in a series of protocols. High standards (as described by Eames, 1999; Menne, 1992; Pitard, 1993; Radford, 1987) in sample transport (drill site to core yard), core cutting, chain of custody and laboratory preparation and analytical techniques were ensured. These protocols followed best practices in quality assurance and quality control (QA/QC), reflecting Barrick global guidelines (based on MRDI (1996) and Stanley (1999)). QA/QC procedures included the insertion of internationally Certified Reference Materials (CRMs), blanks and duplicates to monitor

accuracy, contamination, precision and detect any bias. Different types of duplicates were used to evaluate the reproducibility of core cutting, sample preparation and analytical methods. Monitoring of QC data demonstrated no variation in analytical quality, even though there was a change of laboratory. In addition to a constant and open liaison with the laboratory, the extensive QC program ensured generation of a well constrained and auditable geochemical database.

Shortly after the project demonstrated potential for a significant discovery, the process of generating project matrix-matched CRMs began. Five CRMs were envisioned with concentrations near the likely cut-off grade and certain other strategic points in the population of Au data, along with consideration to Ag and S content. Procedures for generating these QC samples were documented, round-robin data were interpreted and certificates signed by an external Qualified Person. There was no significant cost difference between purchasing commercial CRMs and producing internal matrix-matched material. However, matrix-matched CRMs are considered as current best practice and generated more confidence in the quality of analytical results and, hence, in the grade model.

Multi-element data interpretation and modelling in 3D software was integrated with spectral and geophysical data to further define discrete mineral pulses and alteration paragenesis. A series of cross-sections and level plans assisted in planning the ongoing drill campaign during advanced exploration. These interpretations were also integrated with data from sampling programs along new outcrops resulting from road and drill pad construction. Multi-element 3D geochemical models provided early indications of geometallurgical characteristics of the ore body and waste rock.

An orientation survey was carried out over and through the newly delineated mineral system. This included talus sampling on a grid of 50 x 200 m collected at approximately 40 cm depth and screened at three different size fractions: coarse (<2.0 to >0.177 mm), intermediate (<0.177 to >0.053 mm) and fine (<53 µm). Samples were submitted for analyses of Au by fire assay with ICP-AES (50 g aliquot) and multi-element determinations using low detection digestions and ICP-AES/ICP-MS finish. It was concluded that in this case the most appropriate detection technique for exploration of semi- to concealed Au deposits is analysis of the finest fraction (<53 µm) in talus samples.

As part of the orientation survey, mineral chemistry tools for fertility and vectoring toward high sulfidation deposits from then ongoing research in exploration (e.g. Chang et al., 2011, Cooke et al., 2015 and Zhang et al., 2014) were assessed. Drill core samples were selected for analysis of alunite and quartz by LA-ICP-MS in advanced argillic alteration zones. Results demonstrated paragenesis of several alunite phases and data were consistent with proximity to a large high sulfidation Au deposit. Quartz mineral chemistry indicated mainly hydrothermal replacement-type quartz and data suggested proximity to a large hydrothermal system. Some limitations of these tools were also identified, such as mineral intergrowths, which decrease the amount of data available for interpretation.

Technology to acquire near-real-time data was tested through application of portable X-Ray Fluorescence (pXRF) devices during core logging. The effort was focused on replicating the geochemical signal at the barren/mineralized interface and developing a systematic method to apply while drilling. As such, some elements were found to effectively replicate laboratory results and were applied to drilling procedures for real-time decision making.

GEOPHYSICS

At grassroots scale, during 2010, geophysics played a significant role in the definition of prospective blocks in EIB. Both airborne magnetic and satellite gravity data sets supported and extended the belt-scale structural interpretation at that time, helping to refine major block-bounding structures. Coupled with regional geological mapping, geochronology and other geoscientific data, geophysical interpretations defined the Alturas block as prospective for epithermal high sulfidation mineralization.

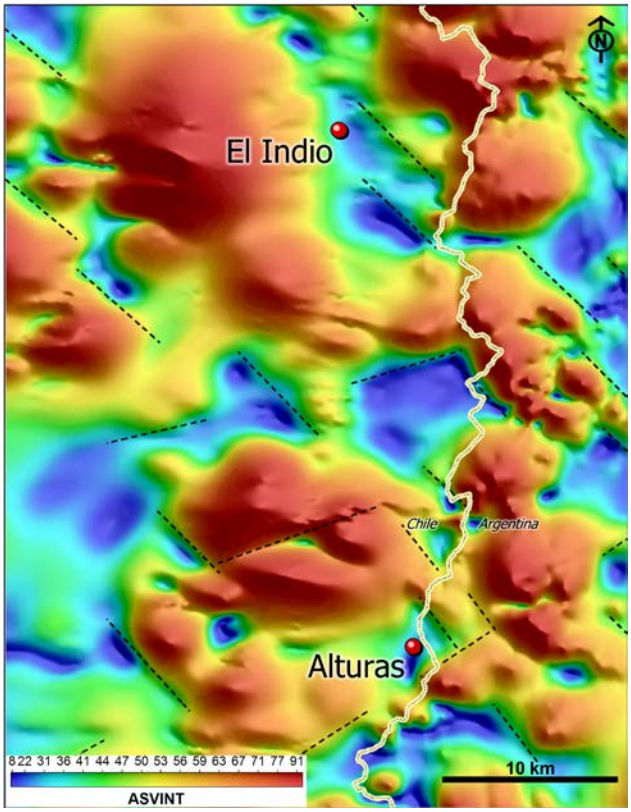

Figure 15: Image of EIB showing the analytic signal of the total magnetic intensity vertical integral (ASVINT). A blue triangular zone (low ASVINT) coincides with extensive hydrothermal alteration at Alturas. Black dashed lines are segments of interpreted lineaments which reflect the underlying structural framework. Chile-Argentina border depicted by yellow-black dashes.

Alturas project is situated north of a major north-east striking lineament in a north-west oriented fabric, both evident in regional magnetic data (Figure 15). These lineaments are interpreted to represent a structural framework developed in

Jurassic-Triassic basement which is usually not directly expressed in Miocene rocks exposed today. However, they likely played an important role in the ascent of magma. Known Andean-scale north/south structures are not apparent in regional aeromagnetic data as they are sub-parallel to flight lines and due to and the Earth's inducing field.

True-color satellite imagery highlights the extensive hydrothermal alteration system that has resulted in significant destruction of magnetite. As expected, the color anomaly is coincident with a pronounced magnetic low at the deposit (Figure 15).

As part of a target delineation program carried out at Alturas, a Controlled Source Audio-MagnetoTelluric (CSAMT) survey was completed. Multiple silicification events significantly raise the inherent resistivity of rocks, especially evident when hosted in less resistive volcanic rocks, a signature typical of high sulfidation Au deposits in EIB. Thus, resistivity methods have been successful as a direct target delineation tool for high sulfidation systems (Goldie, 2000; Teal and Benavides, 2010). CSAMT was selected as the preferred acquisition technique due to its large depth penetration, good lateral resolution, low water requirement and speed of acquisition.

At Alturas, the target area abuts the international border with Argentina and forms a 'pseudo-plateau' of approximately 2.3 km^2 (Figure 16). To best cover the target area as efficiently as possible, receiver dipole lengths were widened to 100 m (compared to an ideal 50 m spacing) on lines initially planned to be 200 m apart. Electrical contact with the ground was achieved via Cu-$CuSO_4$ porous pots in small hand-dug pits. Line orientation of approximately 335° azimuth was selected to be perpendicular to structural directions noted by other workers in the district (Caddy, 2000) and to optimize line length. Three shorter, perpendicular lines were also surveyed to better image any major structure parallel to the main line orientation (Figure 16).

Data acquisition was challenged by difficult access, rugged topography, and impending winter snowfall. The survey commenced on 400 m spaced lines and then in-filled to the planned 200 m line spacing as weather permitted. An aforementioned silicified cliff with 400 m relief which forms the north-west boundary of the pseudo-plateau prohibited continuous data acquisition resulting in several segmented lines. However, the majority of the survey was completed as planned for a total of 14.7 line-km before snow halted progress.

The CSAMT data were acquired in continuous profiling 'scalar' (TM) mode, with each receiver spread typically comprising 6 E_x along-line dipoles and 1 orthogonal H_y measurement. Two grounded dipole transmitters each 2 km in length were located between 6 and 8 km to the north-west and south-east of the survey area. Frequencies in binary steps from 8 – 8192 Hz were used to obtain data to approximately 700 m depth. Data quality was generally considered good, with only a few stations experiencing excessive noise, which were removed from the data set.

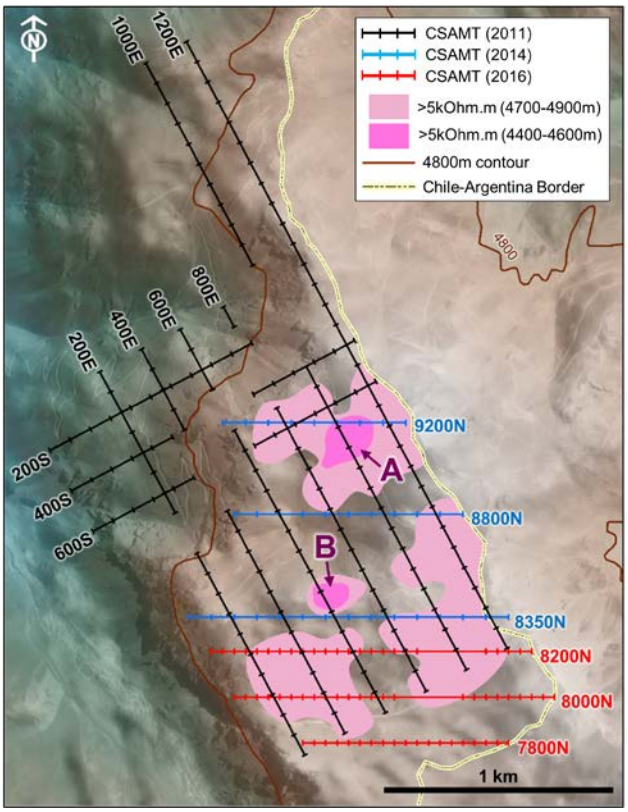

Figure 16: Alturas project area indicating CSAMT surveys by year and early resistive zone interpretation from 1D inversion modelling. Image shows topographic relief which ranges from approximately 3850 – 5150 m. Letters "A" and "B" indicate interpreted feeder zones. Note section 8800N is shown in Figure 17.

Interpretation focused on 1D inversion results, as the 2D sections produced at that time appeared less coherent and did not coincide with interpreted geology. In an attempt to identify blind mineralized centers within an extensive advanced argillic alteration zone, inversion results were classified visually into two classes:

1. Shallow-level – within 300 m of the surface. These zones were interpreted to represent sub-horizontal, tabular, un-mineralized silicification associated with an early acidic fluid pulse.
2. Deep-level – >300 m from the surface. These anomalies were interpreted to be indicators of possible feeder conduit positions.

Two main, deep-rooted silicification centers were identified, one located in the north, adjacent to the highest topographic point, and the other in the center of the project (A and B respectively, Figure 16). The concentric, pervasive form of the northern silicification center (A) and its proximity to mapped steam heated alteration made it the higher priority target. Consequently, two drill holes were planned to test both targets.

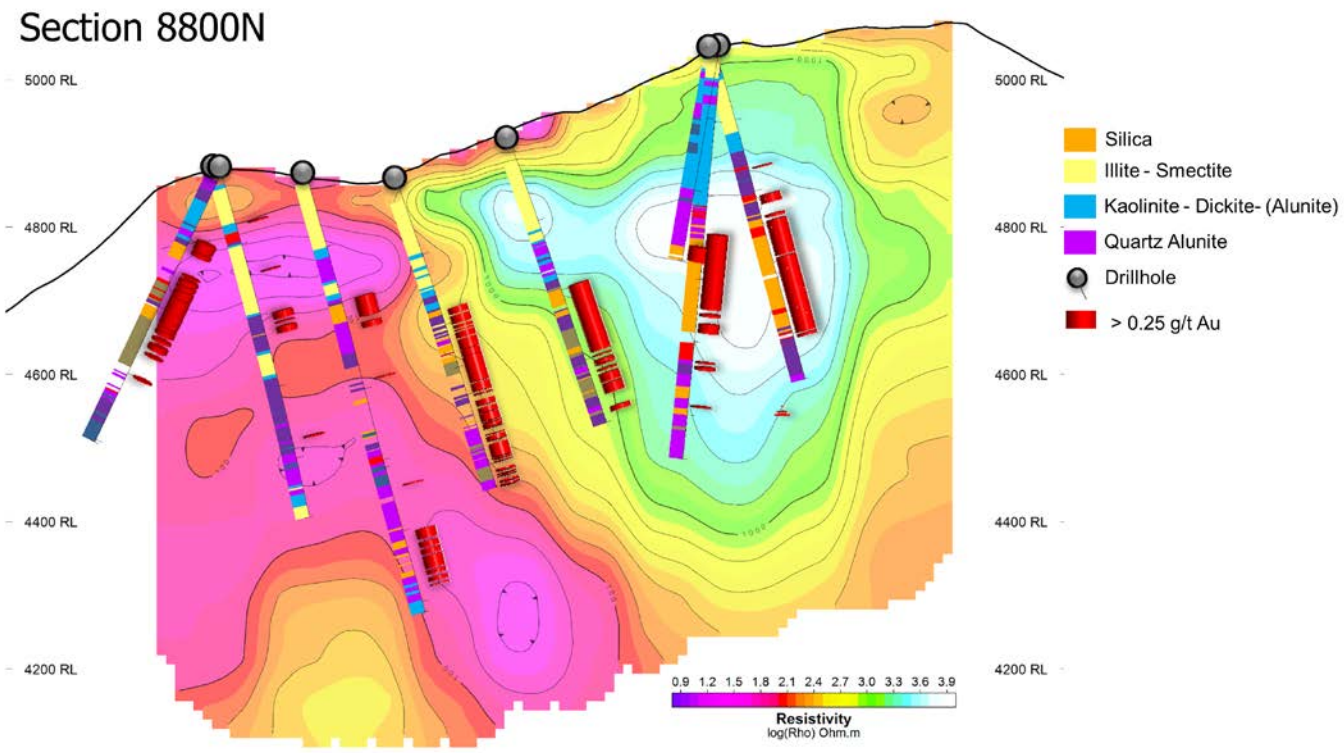

Figure 17: Cross-section 8800 (see Figure 16 for location) showing an imaged 2D CSAMT inversion. Drill hole traces illustrate alteration as various colours and Au mineralized intervals (red bars). Note the correlation between silica alteration in drill hole traces and high resistivity.

As part of drill testing, petrophysical measurements on core samples were collected to characterize alteration and lithology types. An in-house portable desktop laboratory was established to acquire galvanic induced polarization (IP) and resistivity data. Early drilling was confined to an oxide zone and samples returned low IP values. However, later, deeper drilling into a mixed (oxide/sulfide) zone resulted in samples with values typically >30 mV/V. As expected, resistivity measurements on highly silicified samples were complicated by erratic, high contact resistance; however several stable samples reported resistivity values >>5,000 ohm.m.

In response to positive results from initial drill testing, three additional CSAMT lines were acquired in an east-west orientation with 100 m spaced receiver dipoles. These data generally corroborated resistivity anomalies identified in the initial CSAMT program and provided geo-electrical sections directly coincident with the preferred (east-west) drilling orientation.

An example of one of the drill sections is shown in Figure 17. Gold is coincident with several modes of silica – mainly those categorized as brown, grey and vuggy silica. Thickest mineralized intersections occur in a sub-horizontal silicified zone in polymictic rock-flour breccia. Continuous silicified zones are delineated as a CSAMT resistor from the middle of the section toward the east (blue and white colors in Figure 17). Quartz-alunite and illite-smectite alteration dominates the westernmost three drill holes, the effect of which lowers bulk rock resistivity and is clearly represented by the magenta colors in the inversion image (Figure 17). Thin intervals of anomalous gold are largely correlated with brown silica.

As ore body knowledge grew with increasing advanced exploration an additional three lines totaling 3.7 km of CSAMT were acquired. The objective was to detect satellite ore bodies in the southern portion of the pseudo-plateau (Figure 16). Even though an alternative provider acquired data at 50 m receiver dipoles, data quality was compatible to earlier surveys. The new contractor's inversion software produced sections with improved correlation with geology. A subsequent re-processing campaign was undertaken to re-invert all data from previous acquisition stages and this new inversion algorithm was hence adopted as best practice for all CSAMT inversions

CONCLUSIONS

Evolution of the geological understanding which resulted in discovery of Alturas was marked by the application and integration of diverse exploration technologies. This work was led by geoscientists in the areas of geology, spectral geology, geochemistry and geophysics at all scales, from grassroots (2010) to advanced exploration (2015). Each technique was focused on the detection and definition of key geological features which allowed area reduction and vectoring toward ore (Table 2). Grassroots activities in EIB integrated data in such a way as to define prospective structural blocks through understanding stratigraphy of volcanic sequences. Key enablers

were the application of regional geochronology, spectral (Probe 1, ASTER), geochemical (stream sediment and reconnaissance rock chip samples) and geophysical (airborne magnetics and satellite gravity) data sets (Table 2).

Target delineation activities focused follow-up exploration at Alturas during 2011, since it was defined as the area with highest potential to host a mineralized epithermal system. Work at this exploration stage included surface geological mapping at scales of 1:2,500 and 1:1,000 which was focused on identifying features such as a phreatomagmatic environment with development of favorable hydrothermal alteration. Vectoring techniques used at this local scale mainly comprised rock chip sampling over a 2 x 1.5 km area. Geochemical data were interpreted to represent a mineralized horizon 200 m thick, associated with silicification beneath barren cover exhibiting kaolinite-dickite-alunite/illite-smectite alteration (defined by geological mapping and hyperspectral analyses). Further hyperspectral mapping contributed to validating alteration minerals and mineral assemblages and defining compositional indices useful in vectoring to ore. Potential for the presence of a significant volume of silicification was indicated by resistors identified with a CSAMT survey. Integration of these individual target delineation techniques strongly suggested the presence of a phreatomagmatic system with favorable alteration and high potential to host a mineralized system (Figure 18).

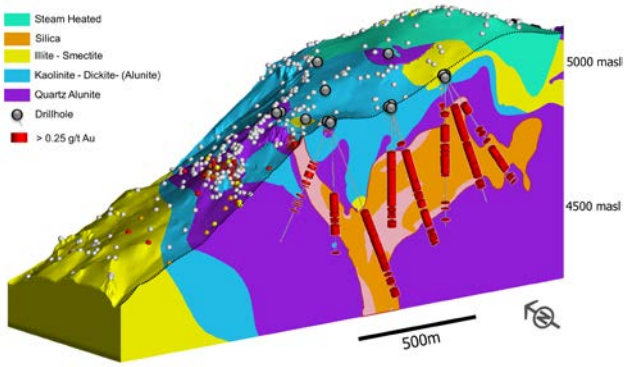

Figure 18: Alteration 3D model derived from integrated geology, spectral data, geochemistry and CSAMT.

Design of a drill testing program was strongly based on surface geology, subtle geochemical trace element anomalies (As-Sb-Bi) and resistors apparent in CSAMT data. Drill testing (2012–2014) aimed to firstly validate the target concept delineated in the previous stage of exploration. Drill results confirmed the predictive geological model with significant intercepts of continuous oxide Au mineralization in a 1 km^2 area under a variable thickness of barren cover (0–200m). This was followed by definition of a geological model focused on understanding the main controls on mineralization such as phreatomagmatic breccias and a favorable horizon.

Advanced exploration commenced (2015) with the objective to establish continuity of, and further define controls on, mineralization and the size and geometry of the ore body. Economic parameters such as strip ratio, metallurgy and preliminary financial aspects (e.g. likely capex, total cash cost, annual production, cashflow) were also estimated. Geological data capture, incorporating geochronological, optical televiewer, Corescan spectral data and multi-element geochemistry of mineralized intercepts led to a validated geological model. This forms the basis of a 3D resource model which is rapidly and frequently updated with a currently inferred resource calculated to be 6.8 Moz at 1 g/t Au.

Appropriate application of exploration techniques (geology, spectral geology, geochemistry and geophysics) in a progressively scale reducing, staged approach, in addition to incorporation of innovative technologies and best practices, has enabled transformation of data to information and, in turn, information to knowledge. These elements are considered fundamental to the success of the project. Nevertheless, the most significant aspect of the Alturas discovery has been collaboration between diverse geoscientists. Field geologists, with the continual support of highly qualified technical specialists and a discovery track record, were motivated to collaborate in a robust, multi-disciplinary, discovery driven team. Global corporate budgetary support for project continuation through the exploration stages and for implementation of new and innovative technologies all contributed to the discovery.

Exploration Stages / Exploration Techniques	GRASSROOTS (GR)	TARGET DELINEATION (TD)	DRILL TESTING (DT)	ADVANCED EXPLORATION (AE)
Geology	Mapping and cross-sections 1:25,000	Mapping and cross-sections 1:2,500 / 1:1,000	Mapping (Roads / Drill pads) and Logging 1:500 / 1:250	Mapping (Roads / Drill pads) and Logging 1:500 / 1:250
Geochronology	Zircon (U-Pb) Lithological	Zircon (U-Pb) Lithological Alunite (K-Ar) Alteration	Zircon (U-Pb) Lithological Alunite (K-Ar) Alteration	Zircon (U-Pb) Lithological Alunite (K-Ar) Alteration
Geochemistry	Stream Sediment Rock Chip	Rock Chip	Core Samples Rock Chip Talus Fine	Core Samples
Remote Sensing	ASTER /SAM	Hand-held SWIR spectrometry	Hand-held SWIR spectrometry	Corescan
Geophysics	Aeromagnetometry	Controlled Source Audio frequency Magnetotelluric (CSAMT)	Controlled Source Audio frequency Magnetotelluric (CSAMT)	Controlled Source Audio frequency Magnetotelluric (CSAMT)
Time (Year)	2010	2011	2012 - 2014	2015 – 2016 (2015 Discovery Announcement)

Table 2: Key exploration techniques employed at the various exploration pipeline stages resulting in the discovery of the Alturas Au deposit.

ACKNOWLEDGEMENTS

The authors would like to thank the organizers of inviting Barrick to contribute to the volume and the Barrick Exploration team responsible for the discovery of Alturas. F. Robert, R. Guerra, M. Gallardo and J. San Vicente are thanked for their constructive comments on an earlier draft of this paper. John Smith ably drafted all the figures. Barrick Gold Corporation is also thanked for permission to publish this paper.

REFERENCES

AusSpec International Ltd. 2012, Spectral Interpretation Field Manual (GMEX –Edition 4).

Barrick, 2017, Barrick Gold Corporation Operations and Technical Update, http://barrick.q4cdn.com/808035602/files/presentation/2017/Barrick-2017-Operations-and-Technical-Update.pdf.

Bissig, T., A. Clark, A. Rainbow, and A. Montgomery, 2015, Physiographic and tectonic setting of high-sulfidation epithermal gold-silver deposits of the Andes and its controls on mineralizing processes: Ore Geology Reviews, 65, 327-364.

Caddy, S., 2000, Interpretive regional fault patterns, tectonic deformation sequence, and regional exploration model, Central Andes Cordillera Chile/Argentina: Confidential report prepared for Homestake Mining Company, 1 – 21.

Camuti, K., 2015, Clay minerals in alteration systems: Terry Leach Symposium, Australian Institute of Geoscientists, Bulletin 48, 13-18.

Chang, Z., J.W. Hedenquist, N.C. White, D.R. Cooke, M. Roach, C.L. Deyell, J. Garcia, J.B. Gemmell, S. McKnight, and A.L. Cuison, 2011, Exploration Tools for Linked Porphyry and Epithermal Deposits: Example from the Mankayan Intrusion-Centered Cu-Au District, Luzon, Philippines: Economic Geology, 106 (8), 1365-1398.

Cooke, D.R., J.J. Wilkinson, M. Baker, P. Agnew, C.C. Wilkinson, H. Martin, Z. Chang, H. Chen, J.B. Gemmell, S. Inglis, L. Danyushevsky, S. Gilbert, and P. Hollings, 2015, Using mineral chemistry to detect the location of concealed porphyry deposits – an example from Resolution: Presented at the 27th International Applied Geochemistry Symposium.

Corbett, G.J. and T.M. Leach, 1998, Southwest Pacific gold-copper systems: Structure, alteration and mineralization: Society of Economic Geologists, Special Publication 6, 238 p.

Eames, J., 1999, Unrealistic expectations of assay results: Good Project – Wrong Assays, Getting Sample Preparation and Assaying Right: Seminar on Quality Assurance in Mineral Assaying (MICA, AusIMM – AIG).

ERSDAC (Earth Remote Sensing Data Analysis Center), 2003, Crosstalk Correction User´s Guide.

Goldie, M., 2000, A geophysical case history of the Yanacocha gold district, northern Perú: 70th Annual International Meeting, SEG, Expanded Abstracts, 750-753.

Hedenquist, J.W., 1987, Mineralization associated with volcanic-related hydrothermal systems in the Circum-Pacific Basin, in M.K. Horn, ed., Circum Pacific Energy and Mineral Resources Conference, 4th, Singapore, 1986, Transactions: American Association of Petroleum Geologists, 513-524.

Heinrich, C.A., 2007, Fluid-Fluid Interactions in Magmatic-Hydrothermal Ore Formation: Reviews in Mineralogy & Geochemistry, 65, 363-387.

Jannas, R.R., T.S. Bowers, P. Ulrich, and R.E. Beane, 1999, High-sulfidation deposit types in the El Indio district, Chile, in B.E. Skinner, ed., Geology and ore deposits of the central Andes, Society of Economic Geologists Special Publication 7, Chapter 7, 219-266.

Menne, D., 1992, Assaying Cyanide Extractable Gold within an Hour, and Addressing Effects of Preg- and Assay-Robbing: Extractive Metallurgy of Gold and Base Metals, Kalgoorlie WA, AusIMM.

MRDI (Mineral Resources Development Inc.), 1996, Assay Quality Assurance-Quality Control Program for Drilling Projects at the Pre-Feasibility to Feasibility Report Level, in D.M. Francois-Bongarçon, S.D. Long, and H.M. Parker eds., 1997 Bankable Ore Reserves and Feasibility Studies, Mineral Resources Development, Inc. San Mateo, California, USA, AIC Conference.

Pitard, F., 1993, Pierre Gy's Sampling Theory and Sampling Practice, Second Edition: CRC Press.

Radford, N.W., 1987, Assessment of error in sampling: Meaningful Sampling in Gold Exploration, Bulletin No 7, 123 p.

Ramos, V.A. and A. Folguera, 2009. Andean flat-slab subduction through time, in J.B. Murphy, J.D. Keppie, and A.J. Hynes, eds., Ancient Orogens and Modern Analogues, Geological Society, London, Special Publications, 327, 31–54.

Sillitoe, R.H., 1999, Styles of high-sulphidation gold, silver and copper mineralization in porphyry and epithermal environments: Pacrim '99, 29-44.

Sillitoe, R.H. and J.W. Hedenquist, 2003, Linkages between volcanotectonic settings, ore-fluid compositions, and epithermal precious-metal deposits, in S.F. Simmons and I.J. Graham, eds., Volcanic, geothermal and ore-forming fluids: Rulers and witnesses of processes within the Earth, Society of Economic Geologists and Geochemical Society, Special Publication 10, Chapter 16, 315-343.

Stanley, C.R., 1999, Treatment of Geochemical Data: Some Pitfalls in Graphical Analysis: Quality Control in Mineral Exploration, Short Course, 19th IGES, Association of Exploration Geochemists.

Teal, L. and A. Benavides, 2010, History and geologic overview of the Yanacocha mining district, Cajamarca, Perú: Economic Geology, 105 (7), 1173 – 1190.

Zhang, L., N. White, J.A. Thompson, M.J. Baker, D.R. Cooke, and H. Chen, 2014, Lithocap blind test site - Barrick, AMIRA, Hobart, Australia, P1060, Contract Report.